Application of the Eigenmode Transformation Technique for the Analysis of Planar Transmission Lines

Christian Rieckmann, Andreas Jöstingmeier, and A. S. Omar, *Senior Member, IEEE*

Abstract—**The eigenmode transformation technique is formulated for the analysis of inhomogeneously filled shielded waveguides containing metal inserts. The permittivity of the filling medium may be an arbitrary function of the transverse coordinates. The method is based on expanding the electromagnetic field in terms of the eigenmodes of the corresponding empty shielding waveguide. The metal inserts have first the effect of linearly transforming the eigenmodes of the empty guide into those of the shielded waveguide containing the metal inserts (including the TEM-modes). Next the inhomogeneity of the filling medium is taken into account which leads to a proper matrix eigenvalue problem. In addition an alternative formulation is derived from a variational approach. Results of both formulations are compared for a shielded circular dielectric waveguide. The eigenmode transformation technique is applied to various types of planar transmission lines, i.e., coupled microstrip lines, finlines, and coplanar lines. The results are compared with those of other methods.**

I. Introduction

We consider the inhomogeneously filled waveguide shown in Fig. 1. The inhomogeneity is given by a permittivity which may be an arbitrary function of the transverse coordinates and the waveguide may contain one or more metal inserts. Such a waveguide represents, e.g., shielded coupled microstrip lines, finlines or shielded dielectric image guides. In the analysis of microwave components, e.g., waveguide discontinuities or junctions, a large number of eigenmodes of the corresponding waveguides are needed to achieve a sufficiently high accuracy. As has been shown in [1] it is mandatory that no low order eigenmodes are overlooked. This is a crucial aspect because in general the waveguides considered support complex eigenmodes [2]–[4]. Due to the geometrical similarity of different types of transmission lines (e.g., there is no essential difference between the dielectric substrate of a finline and that of a microstrip line), it would be desirable to have a modular method at hand. This means that once the eigenmode coupling corresponding to a dielectric substrate has been calculated the results can be used for various line types based on this substrate.

Manuscript received March 27, 1996. This work was supported by the Deutsche Forschungsgemeinschaft.

C. Rieckmann and A. S. Omar are with the Technische Universität Hamburg–Harburg, Arbeitsbereich Hochfrequenztechnik, Wallgraben 55, D-21071 Hamburg, Germany.

A. Jöstingmeier is with the Deutsches Elektronen–Synchrotron (DESY), Notkestr. 85, D-22607 Hamburg, Germany.

Publisher Item Identifier S 0018-9480(96)08553-5.

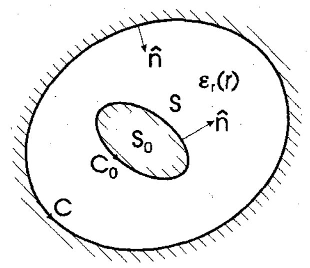

Fig. 1. Cross section of an inhomogeneously filled shielded waveguide.

Although the method presented in [5] leads to a proper matrix eigenvalue problem, to the authors' best knowledge it has not yet been applied to the actual computation of eigenmodes. Conventional approaches result in a homogeneous system of equations given by a characteristic matrix, the elements of which are functions of the yet unknown propagation constant [6]. For a nontrivial solution the characteristic matrix becomes singular. This is not a proper matrix eigenvalue problem. Each eigenvalue has to be found as a complex zero of the determinant corresponding to the characteristic matrix. On the other hand, the solution of a proper eigenvalue problem yields a large number of eigenvalues (corresponding to the size of the characteristic matrix) at once.

As has been shown in [7], the set of TE- and TM-eigenmodes corresponding to an empty waveguide is complete if no *a-priori* coupling between the field components of these eigenmodes is assumed. On the other hand for waveguides with metal inserts additionally to the TE- and TM-eigenmodes one or more TEM-eigenmodes (equal to the number of metal inserts) have to be taken into account to form a complete set. In this contribution we will follow the analysis of [5] by expanding the field of the inhomogeneously filled waveguide in terms of the eigenmodes of the corresponding empty waveguide. In [8] it has been demonstrated that TM- and TEM-eigenmodes of a waveguide with metal inserts can be expressed in terms of the TM-eigenmodes of the corresponding empty waveguide; whereas the TE-eigenmodes are linear combinations of TE- and TM-eigenmodes. The influence of metal inserts can then be described by a linear transformation of the matrices constituting the eigenvalue problem corresponding to the shielding waveguide with dielectric only. This results in a new proper matrix eigenvalue problem. The computation of the transformation matrices can be treated as a separate problem [8]–[10] what leads to a modular character of the method.

II. Theory

Referring to Fig. 1, the cross section (contour) of the shielding waveguide and that of the metal insert are denoted by S (C) and S_0 (C_0), respectively. The unit vector normal to C and C_0 is represented by $\hat{\boldsymbol{n}}$. The permittivity ϵ_r is a function of the transverse coordinates $\boldsymbol{r}$. The direction of propagation, in which the structure is uniform, is taken along the z-axis with a corresponding propagation constant β.

Let $\{\mathcal{H}_{zn}\}$ and $\{\mathcal{E}_{zn}\}$ be the complete sets of axial magnetic and axial electric fields characterizing the TE- and TM-eigenmodes, respectively, corresponding to the waveguide according to Fig. 1 without dielectric. Due to the existence of N isolated metal inserts there exist N linearly independent potential functions Φ_n which describe the corresponding TEM-modes. $\mathcal{H}_{zn}, \mathcal{E}_{zn}$, and Φ_n are real functions of the transverse coordinates which correspond to cut-off wavenumbers κ_n^h, κ_n^e, and 0, respectively. They satisfy the orthogonality relations

$$\int_{S-S_0} \mathcal{H}_{zn}\mathcal{H}_{zm}\, dS = \frac{1}{(\kappa_n^h)^2}\delta_{nm} \tag{1a}$$

$$\int_{S-S_0} \mathcal{E}_{zn}\mathcal{E}_{zm}\, dS = \frac{1}{(\kappa_n^e)^2}\delta_{nm} \tag{1b}$$

$$\int_{S-S_0} \nabla_t\Phi_n \cdot \nabla_t\Phi_m\, dS = \delta_{nm} \tag{1c}$$

where δ_{nm} is the Kronecker delta and ∇_t is the transverse component of the del-operator. Note that $\mathcal{H}_{zn}, \mathcal{E}_{zn}$, and Φ_n are defined over $S - S_0$ only.

A. Eigenmode Transformation Technique

Let $\hat{\boldsymbol{k}}$ be the unit vector in axial direction. The sets $\{\nabla_t\mathcal{H}_{zn} \times \hat{\boldsymbol{k}}\}$ and $(\{\nabla_t\mathcal{E}_{zn}\}, \{\nabla_t\Phi_n\})$ are complete with respect to divergence-free and curl-free transverse electric fields, respectively. The sets $(\{\hat{\boldsymbol{k}} \times \nabla_t\mathcal{E}_{zn}\}, \{\hat{\boldsymbol{k}} \times \nabla_t\Phi_n\})$ and $\{\nabla_t\mathcal{H}_{zn}\}$ have the same properties with respect to the magnetic field. Let $\boldsymbol{E}_t, \boldsymbol{H}_t, E_z$, and H_z be the transverse electric, transverse magnetic, axial electric, and axial magnetic field components, respectively, then we can write

$$\epsilon_r\boldsymbol{E}_t = \sum_n^\infty U_n^H(\nabla_t\mathcal{H}_{zn} \times \hat{\boldsymbol{k}}) + \sum_n^\infty U_n^E\nabla_t\mathcal{E}_{zn} + \sum_{n=1}^N U_n^0\nabla_t\Phi_n \tag{2a}$$

$$\boldsymbol{H}_t = \sum_n^\infty I_n^H\nabla_t\mathcal{H}_{zn} + \sum_n^\infty I_n^E(\hat{\boldsymbol{k}} \times \nabla_t\mathcal{E}_{zn}) + \sum_{n=1}^N I_n^0(\hat{\boldsymbol{k}} \times \nabla_t\Phi_n) \tag{2b}$$

$$\epsilon_r E_z = \sum_n^\infty U_n^L\kappa_n^e\mathcal{E}_{zn} \tag{2c}$$

$$H_z = \sum_n^\infty I_n^L\kappa_n^h\mathcal{H}_{zn} \tag{2d}$$

where the z-dependence $e^{-j\beta z}$ has been dropped out for all field components.

Let $\{h_{zn}\}$ and $\{e_{zn}\}$ denote the complete sets of axial magnetic and axial electric fields belonging to the TE- and TM-eigenmodes, respectively, corresponding to the empty shielding waveguide. For e_{zn} and h_{zn}, orthogonality relations corresponding to (1a) and (1b) are valid with cutoff wavenumbers k_n^e and k_n^h, respectively. Inside a metal insert, the electromagnetic field vanishes. Since e_{zn} and h_{zn} are defined everywhere over S, we can expand the fields given by $(\nabla_t\mathcal{E}_{zi}, \nabla_t\Phi_i), \nabla_t\mathcal{H}_{zi}, \mathcal{E}_{zi}$, and $\mathcal{H}_{zi}$ over $S - S_0$ and by zero over S_0 with respect to $\nabla_t e_{zp}, (\nabla_t h_{zp}, (\hat{\boldsymbol{k}} \times \nabla_t e_{zp})), e_{zp}$, and h_{zp}, respectively [8]

$$\sum_p^\infty \mathcal{U}_{pi}^{EE}\nabla_t e_{zp} = \begin{cases} \nabla_t\mathcal{E}_{zi} & \text{over } S - S_0 \\ \boldsymbol{o} & \text{over } S_0 \end{cases} \tag{3a}$$

$$\sum_p^\infty \mathcal{U}_{pi}^{E0}\nabla_t e_{zp} = \begin{cases} \nabla_t\Phi_i & \text{over } S - S_0 \\ \boldsymbol{o} & \text{over } S_0 \end{cases} \tag{3b}$$

$$\sum_p^\infty \mathcal{J}_{pi}^{HH}\nabla_t h_{zp} + \sum_p^\infty \mathcal{J}_{pi}^{EH}(\hat{\boldsymbol{k}} \times \nabla_t e_{zp}) = \begin{cases} \nabla_t\mathcal{H}_{zi} & \text{over } S - S_0 \\ \boldsymbol{o} & \text{over } S_0 \end{cases} \tag{3c}$$

$$\sum_p^\infty \mathcal{U}_{pi}^L k_p^e e_{zp} = \begin{cases} \kappa_i^e\mathcal{E}_{zi} & \text{over } S - S_0 \\ 0 & \text{over } S_0 \end{cases} \tag{3d}$$

$$\sum_p^\infty \mathcal{J}_{pi}^L k_p^h h_{zp} = \begin{cases} \kappa_i^h\mathcal{H}_{zi} & \text{over } S - S_0 \\ 0 & \text{over } S_0. \end{cases} \tag{3e}$$

Let us denote the field given by the right-hand side of (3c) with $\boldsymbol{\mathcal{H}}_t$. Because the tangential component of $\boldsymbol{\mathcal{H}}_t$ has a step discontinuity at $C_0, (\nabla_t \times \boldsymbol{\mathcal{H}}_t)$ which includes the normal derivative of the tangential component behaves as a Dirac delta function there. This Dirac delta function is just the axial component of the surface current at C_0. The vector $(\nabla_t \times \boldsymbol{\mathcal{H}}_t)$ then vanishes everywhere over S except at C_0, and hence $\boldsymbol{\mathcal{H}}_t$ cannot be expanded in terms of the curl-free set $\{\nabla_t h_{zp}\}$ only. It needs, in addition, the divergence-free set $\{\hat{\boldsymbol{k}} \times \nabla_t e_{zp}\}$. On the other hand, the functions defined by the right-hand side of (3a) and (3b), respectively, can be expanded in terms of the curl-free set $\{\nabla_t e_{zp}\}$ because the tangential component of these functions is continuous across C_0.

Substituting the field representations according to (2a)–(2d) into Maxwell's equations and making use of the orthogonality properties (1a)–(1c), we arrive at

$$\frac{\tilde{\kappa}_n^e}{j\tilde{\beta}}\sum_i^\infty \mathcal{S}_{ni}U_i^L + \sum_i^\infty \mathcal{R}_{ni}^{ee}U_i^E + \sum_{i=1}^N \mathcal{R}_{ni}^{e0}U_i^0 + \sum_i^\infty \mathcal{T}_n U_i^H = \frac{Z_0}{\tilde{\beta}}I_n^E \tag{4a}$$

$$\sum_i^\infty \mathcal{T}_{in}U_i^E + \sum_{i=1}^N \mathcal{T}_{in}^0 U_i^0 + \sum_i^\infty \mathcal{R}_{ni}^{hh}U_i^H = \frac{-jZ_0}{\tilde{\kappa}_n^H}I_n^L \tag{4b}$$

$$\sum_i^\infty \mathcal{R}_{in}^{e0}U_i^E + \sum_{i=1}^N \mathcal{R}_{ni}^{00}U_i^0 + \sum_i^\infty \mathcal{T}_{ni}^0 U_i^H = \frac{Z_0}{\tilde{\beta}}I_n^0 \tag{4c}$$

$$\sum_i^{\infty} \mathcal{T}_{in} U_i^E + \sum_{i=1}^{N} \mathcal{T}_{in}^0 U_i^0 + \sum_i^{\infty} \mathcal{R}_{ni}^{hh} U_i^H = \frac{Z_0}{\tilde{\beta}} I_n^H \tag{4d}$$

$$I_n^E = \frac{-j}{\tilde{\kappa}_n^e Z_0} U_n^L \tag{4e}$$

$$\tilde{\kappa}_n^h I_n^L + j\tilde{\beta} I_n^H = \frac{j}{Z_0} U_n^H \tag{4f}$$

$$\tilde{\beta} I_n^E = \frac{1}{Z_0} U_n^E \tag{4g}$$

$$\tilde{\beta} I_n^0 = \frac{1}{Z_0} U_n^0 \tag{4h}$$

where Z_0 is the intrinsic impedance of free space. Quantities marked with a tilde ($\tilde{}$) are normalized to the free space wavenumber k_0. The coupling integrals $\mathcal{R}_{ij}^{hh}, \mathcal{R}_{ij}^{ee}, \mathcal{R}_{ij}^{e0}, \mathcal{R}_{ij}^{00}, \mathcal{T}_{ij}, \mathcal{T}_{ij}^0$, and $\mathcal{S}_{ij}$ read

$$\mathcal{R}_{ij}^{hh} = \int_{S-S_0} \frac{\nabla_t \mathcal{H}_{zi} \cdot \nabla_t \mathcal{H}_{zj}}{\epsilon_r} \, dS \tag{5a}$$

$$\mathcal{R}_{ij}^{ee} = \int_{S-S_0} \frac{\nabla_t \mathcal{E}_{zi} \cdot \nabla_t \mathcal{E}_{zj}}{\epsilon_r} \, dS \tag{5b}$$

$$\mathcal{R}_{ij}^{e0} = \int_{S-S_0} \frac{\nabla_t \mathcal{E}_{zi} \cdot \nabla_t \Phi_j}{\epsilon_r} \, dS \tag{5c}$$

$$\mathcal{R}_{ij}^{00} = \int_{S-S_0} \frac{\nabla_t \Phi_i \cdot \nabla_t \Phi_j}{\epsilon_r} \, dS \tag{5d}$$

$$\mathcal{T}_{ij} = \int_{S-S_0} \frac{(\nabla_t \mathcal{E}_{zi} \times \nabla_t \mathcal{H}_{zj}) \cdot \hat{\boldsymbol{k}}}{\epsilon_r} \, dS \tag{5e}$$

$$\mathcal{T}_{ij}^0 = \int_{S-S_0} \frac{(\nabla_t \Phi_i \times \nabla_t \mathcal{H}_{zj}) \cdot \hat{\boldsymbol{k}}}{\epsilon_r} \, dS \tag{5f}$$

$$\mathcal{S}_{ij} = \kappa_i^e \kappa_j^e \int_{S-S_0} \frac{\mathcal{E}_{zi} \mathcal{E}_{zj}}{\epsilon_r} \, dS. \tag{5g}$$

Substituting the series representations for $\nabla_t \mathcal{H}_{zi}, \nabla_t \mathcal{E}_{zi}, \nabla_t \Phi_i$, and $\mathcal{E}_{zi}$ according to (3a)–(3d) into (5a)–(5g), the integrals can be extended over S. This is possible because the series are defined over this region; and they vanish over S_0. In matrix notation, we get the coupling matrices $[\mathcal{R}^{hh}], [\mathcal{R}^{ee}], [\mathcal{R}^{e0}], [\mathcal{R}^{00}], [\mathcal{T}], [\mathcal{T}^0]$, and $[\mathcal{S}]$ containing the elements $\mathcal{R}_{ij}^{hh}, \mathcal{R}_{ij}^{ee}, \mathcal{R}_{ij}^{e0}, \mathcal{R}_{ij}^{00}, \mathcal{T}_{ij}, \mathcal{T}_{ij}^0$, and $\mathcal{S}_{ij}$, respectively, as a linear transformation of the matrices $[R^h], [R^e], [T]$, and $[S]$

$$[\mathcal{R}^{hh}] = [[\mathcal{J}^{HH}]^t, [\mathcal{J}^{EH}]^t] \cdot \begin{bmatrix} [R^h] & [T]^t \\ [T] & [R^e] \end{bmatrix} \begin{bmatrix} [\mathcal{J}^{HH}] \\ [\mathcal{J}^{EH}] \end{bmatrix} \tag{6a}$$

$$\begin{bmatrix} [\mathcal{R}^{ee}] & [\mathcal{R}^{e0}] \\ [\mathcal{R}^{e0}]^t & [\mathcal{R}^{00}] \end{bmatrix} = \begin{bmatrix} [\mathcal{U}^{EE}]^t \\ [\mathcal{U}^{E0}]^t \end{bmatrix} [R^e][[\mathcal{U}^{EE}], [\mathcal{U}^{E0}]] \tag{6b}$$

$$\begin{bmatrix} [\mathcal{T}] \\ [\mathcal{T}^0] \end{bmatrix} = \begin{bmatrix} [\mathcal{U}^{EE}]^t \\ [\mathcal{U}^{E0}]^t \end{bmatrix} [[T], [R^e]] \begin{bmatrix} [\mathcal{J}^{HH}] \\ [\mathcal{J}^{EH}] \end{bmatrix} \tag{6c}$$

$$[\mathcal{S}] = [\mathcal{U}^L]^t [S] [\mathcal{U}^L]. \tag{6d}$$

The elements of $[R^h], [R^e], [T]$, and $[S]$ are given by

$$R_{ij}^h = \int_{S-S_0} \frac{\nabla_t h_{zi} \cdot \nabla_t h_{zj}}{\epsilon_r} \, dS \tag{7a}$$

$$R_{ij}^e = \int_{S-S_0} \frac{\nabla_t e_{zi} \cdot \nabla_t e_{zj}}{\epsilon_r} \, dS \tag{7b}$$

$$T_{ij} = \int_{S-S_0} \frac{(\nabla_t e_{zi} \times \nabla_t h_{zj}) \cdot \hat{\boldsymbol{k}}}{\epsilon_r} \, dS \tag{7c}$$

$$S_{ij} = k_i^e k_j^e \int_{S-S_0} \frac{e_{zi} e_{zj}}{\epsilon_r} \, dS. \tag{7d}$$

The matrices $[R^h], [R^e], [T]$, and $[S]$ characterize the coupling of the eigenmodes corresponding to the empty shielded waveguide by the dielectric. Due to the metal insert, a linear transformation of these matrices has to be carried out. The transformation matrices $[\mathcal{J}^{HH}], [\mathcal{J}^{EH}], [\mathcal{U}^{EE}], [\mathcal{U}^{E0}]$, and $[\mathcal{U}^L]$ contain the elements $\mathcal{J}_{pi}^{HH}, \mathcal{J}_{pi}^{EH}, \mathcal{U}_{pi}^{EE}, \mathcal{U}_{pi}^{E0}$, and $\mathcal{U}_{pi}^L$, respectively, which are given by (3a)–(3d). Note that waveguides which are based on the same substrate are described by identical matrices $[R^h], [R^e], [T]$, and $[S]$.

If use is made of (4a)–(4h) all expansion coefficients except for U_i^E, U_i^0, and U_i^H can be eliminated. One arrives then at a proper matrix eigenvalue problem

$$\begin{bmatrix} [I] - [\tilde{\kappa}^h]^2[\mathcal{R}^{hh}] & -[\tilde{\kappa}^h]^2[\mathcal{T}]^t & -[\tilde{\kappa}^h]^2[\mathcal{T}^0]^t \\ [0] & [I] - [\tilde{\kappa}^e][\mathcal{S}][\tilde{\kappa}^e] & [0] \\ [0] & [0] & [I] \end{bmatrix} \begin{pmatrix} \boldsymbol{U}^H \\ \boldsymbol{U}^E \\ \boldsymbol{U}^0 \end{pmatrix} = (\tilde{\beta})^2 \begin{bmatrix} [\mathcal{R}^{hh}] & [\mathcal{T}]^t & [\mathcal{T}^0]^t \\ [\mathcal{T}] & [\mathcal{R}^{ee}] & [\mathcal{R}^{e0}] \\ [\mathcal{T}^0] & [\mathcal{R}^{e0}]^t & [\mathcal{R}^{00}] \end{bmatrix} \begin{pmatrix} \boldsymbol{U}^H \\ \boldsymbol{U}^E \\ \boldsymbol{U}^0 \end{pmatrix}. \tag{8}$$

The unit and the zero matrices are denoted by $[I]$ and $[0]$, respectively. The column vectors $\boldsymbol{U}^H, \boldsymbol{U}^E$, and $\boldsymbol{U}^0$ contain the elements U_n^H, U_n^E, and U_n^0, respectively. The eigenvalues are the normalized propagation constants squared. Since in (8) all matrix elements are real the eigenvalues are either real or form complex-conjugate pairs. The matrix at the right-hand side of (8) is symmetric and does not depend on the free space wavenumber k_0. Corresponding statements are not valid for the matrix at the left-hand side. Note that none of the submatrices has to be inverted or must be multiplied with another nondiagonal submatrix. In view of the numerical implementation of (8), this advantage results from the expansion of $\epsilon_r \boldsymbol{E}$ instead of $\boldsymbol{E}$.

The electromagnetic field of an eigenmode of the structure shown in Fig. 1 is determined by the corresponding eigenvectors $(\boldsymbol{U}^H)^t$, $(\boldsymbol{U}^E)^t$, and $(\boldsymbol{U}^0)^t)^t$. E.g., the transverse electric field can be represented in terms of the known TM- and TE-eigenmodes corresponding to the empty shielded waveguide by

$$\epsilon_r \boldsymbol{E}_t = e^{-j\beta z} \left(\sum_i^{\infty} u_i^E \nabla_t e_{zi} + \sum_i^{\infty} u_i^H (\nabla_t h_{zi} \times \hat{\boldsymbol{k}}) \right). \tag{9a}$$

The expansion coefficients u_i^E and u_i^H are related to an eigenvector of (8) by

$$\boldsymbol{u}^E = [\mathcal{U}^{EE}]\boldsymbol{U}^E + [\mathcal{U}^{E0}]\boldsymbol{U}^0 + [\mathcal{J}^{EH}]\boldsymbol{U}^H \tag{9b}$$

$$\boldsymbol{u}^H = [\mathcal{J}^{HH}]\boldsymbol{U}^H \tag{9c}$$

where $\boldsymbol{u}^E$ and $\boldsymbol{u}^H$ denote column vectors containing the elements u_i^E and u_i^H, respectively. The other field components can be deduced using some of the relations of (4a)–(4h).

B. Variational Approach

In this subsection another approach for the analysis of inhomogeneously filled shielded waveguides is presented, based on a variational expression for β^2 [11], [12]. The Rayleigh–Ritz procedure is then applied in order to determine the corresponding electromagnetic field.

The electric field in an inhomogeneously filled dielectric waveguide satisfies the vector wave equation

$$\nabla \times \nabla \times \boldsymbol{E} - \epsilon_r k_0^2 \boldsymbol{E} = \boldsymbol{o}. \tag{10}$$

Assuming an $e^{-j\beta z}$-dependence of the electric field, (10) can be seperated into its transverse and axial components. Using the fact that the divergence of the flux density $\boldsymbol{D}$ vanishes, the axial electric field can be eliminated

$$\hat{\boldsymbol{k}} \times \nabla_t \times \nabla_t \times \boldsymbol{E}_t - \hat{\boldsymbol{k}} \times \nabla_t \frac{1}{\epsilon_r} \nabla_t \cdot \epsilon_r \boldsymbol{E}_t - \epsilon_r k_0^2 \hat{\boldsymbol{k}} \times \boldsymbol{E}_t + \beta^2 \hat{\boldsymbol{k}} \times \boldsymbol{E}_t = \boldsymbol{o}. \tag{11}$$

Equation (11) is an eigenvalue equation which can be written in operator notation

$$\mathcal{L}_e \boldsymbol{E}_t = \beta^2 \mathcal{B} \boldsymbol{E}_t \tag{12a}$$

with the linear differential operators

$$\mathcal{L}_e = \hat{\boldsymbol{k}} \times \nabla_t \times \nabla_t \times -\hat{\boldsymbol{k}} \times \nabla_t \frac{1}{\epsilon_r} \nabla_t \cdot \epsilon_r - \epsilon_r k_0^2 \tag{12b}$$

$$\mathcal{B} = -\hat{\boldsymbol{k}} \times . \tag{12c}$$

In [12] it has been shown that $\mathcal{L}_e$ and $\mathcal{B}$ are neither symmetric nor self-adjoint, while the adjoint operators of $\mathcal{L}_e$ and $\mathcal{B}$ have to fulfill the vector wave equation of the magnetic field. This gives rise to a variational expression for β^2

$$\beta^2 = -\frac{\langle \boldsymbol{H}_t, \mathcal{L}_e \boldsymbol{E}_t \rangle}{\langle \boldsymbol{H}_t, \mathcal{B} \boldsymbol{E}_t \rangle} \tag{13}$$

where the $\langle f, g \rangle$-notation denotes the inner product of the two functions f and g. After some mathematical manipulations one arrives at

$$\beta^2 = \frac{1}{\langle \boldsymbol{H}_t, \hat{\boldsymbol{k}} \times \boldsymbol{E}_t \rangle} \cdot \left(\langle \hat{\boldsymbol{k}} \nabla_t \cdot \boldsymbol{H}_t, \nabla_t \times \boldsymbol{E}_t \rangle - \left\langle \frac{1}{\epsilon_r} \nabla_t \times \boldsymbol{H}_t, \hat{\boldsymbol{k}} \nabla_t \cdot \epsilon \boldsymbol{E}_t \right\rangle + k_0^2 \langle \boldsymbol{H}_t, \hat{\boldsymbol{k}} \times \epsilon_r \boldsymbol{E}_t \rangle \right). \tag{14}$$

Up to this point our analysis went parallel to that of [12].

Let us now expand the transverse electric field with respect to the complete sets $\{\nabla_t \mathcal{H}_{zn} \times \hat{\boldsymbol{k}}\}, \{\nabla_t \mathcal{E}_{zn}\}$, and $\{\nabla_t \Phi_n\}$

$$\boldsymbol{E}_t = \sum_n^{\infty} V_n^H (\nabla_t \mathcal{H}_{zn} \times \hat{\boldsymbol{k}}) + \sum_n^{\infty} V_n^E \nabla_t \mathcal{E}_{zn} + \sum_{n=1}^{N} V_n^0 \nabla_t \Phi_n \tag{15}$$

while for the expansion of the transverse magnetic field (2b) can be used. Using some vector algebra yields

$$\nabla_t \cdot \boldsymbol{H}_t = -\sum_n^{\infty} I_n^H (\kappa_n^h)^2 \mathcal{H}_{zn} \tag{16a}$$

$$\nabla_t \times \boldsymbol{E}_t = \sum_n^{\infty} V_n^H (\kappa_n^h)^2 \mathcal{H}_{zn} \hat{\boldsymbol{k}} \tag{16b}$$

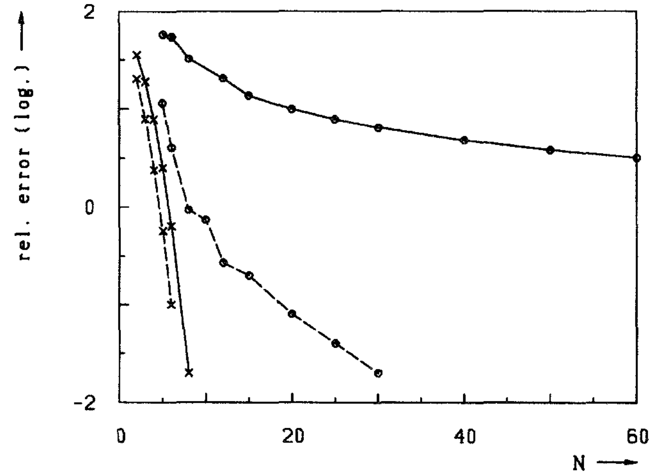

Fig. 2. Convergence of eigenvalues for a shielded circular dielectric waveguide; —— (– –): solution of (8) (19)); o (×): step-index (gaussian)-profile.

$$\nabla_t \times \boldsymbol{H}_t = -\sum_n^{\infty} I_n^E (\kappa_n^e)^2 \mathcal{E}_{zn} \hat{\boldsymbol{k}} \tag{16c}$$

$$\nabla_t \cdot \epsilon_r \boldsymbol{E}_t = -\epsilon_r \sum_n^{\infty} V_n^E (\kappa_n^e)^2 \mathcal{E}_{zn} + \nabla_t \epsilon_r \sum_n^{\infty} V_n^H (\nabla_t \mathcal{H}_{zn} \times \hat{\boldsymbol{k}}) + \nabla_t \epsilon_r \sum_n^{\infty} V_n^E \nabla_t \mathcal{E}_{zn} + \nabla_t \epsilon_r \sum_{n=1}^{N} V_n^0 \nabla_t \Phi_n. \tag{16d}$$

Integrating over $S - S_0$ the inner products required in (14) can be evaluated leading to

$$\langle \hat{\boldsymbol{k}} \nabla_t \cdot \boldsymbol{H}_t, \nabla_t \times \boldsymbol{E}_t \rangle = -(\boldsymbol{I}^H)^t [\kappa^h]^2 \boldsymbol{V}^H \tag{17a}$$

$$\left\langle \frac{1}{\epsilon_r} \nabla_t \times \boldsymbol{H}_t, \hat{\boldsymbol{k}} \nabla_t \cdot \epsilon \boldsymbol{E}_t \right\rangle = (\boldsymbol{I}^E)^t [\kappa^e]^2 (([I] - [\mathcal{W}]) \boldsymbol{V}^E + ([I] - [\mathcal{W}^0]) \boldsymbol{V}^0 - [\mathcal{V}] \boldsymbol{V}^H) \tag{17b}$$

$$\begin{aligned} \langle \boldsymbol{H}_t, \hat{\boldsymbol{k}} \times \epsilon_r \boldsymbol{E}_t \rangle &= (\boldsymbol{I}^H)^t ([\overline{\mathcal{R}}^{hh}] \boldsymbol{V}^H + [\overline{\mathcal{T}}]^t \boldsymbol{V}^E + [\overline{\mathcal{T}}^0]^t \boldsymbol{V}^0) \\ &+ (\boldsymbol{I}^E)^t ([\overline{\mathcal{T}}] \boldsymbol{V}^H + [\overline{\mathcal{R}}^{ee}] \boldsymbol{V}^E + [\overline{\mathcal{R}}^{e0}] \boldsymbol{V}^0) \\ &+ (\boldsymbol{I}^0)^t ([\overline{\mathcal{T}}^0] \boldsymbol{V}^H + [\overline{\mathcal{R}}^{e0}]^t \boldsymbol{V}^E + [\overline{\mathcal{R}}^{00}] \boldsymbol{V}^0) \end{aligned} \tag{17c}$$

$$\langle \boldsymbol{H}_t, \hat{\boldsymbol{k}} \times \boldsymbol{E}_t \rangle = (\boldsymbol{I}^H)^t \boldsymbol{V}^H + (\boldsymbol{I}^E)^t \boldsymbol{V}^E + (\boldsymbol{I}^0)^t \boldsymbol{V}^0. \tag{17d}$$

The bar ($\overline{\ }$) denotes that (5a)–(5g) are to be computed with $1/\epsilon_r$ being replaced by ϵ_r. The matrices $[\mathcal{V}], [\mathcal{W}]$, and $[\mathcal{W}^0]$, respectively, contain the elements

$$\mathcal{V}_{ij} = -\int_{S-S_0} \ln \epsilon_r (\nabla_t \mathcal{E}_{zi} \times \nabla_t \mathcal{H}_{zj}) \cdot \hat{\boldsymbol{k}} \, dS \tag{18a}$$

$$\mathcal{W}_{ij}^0 = -\int_{S-S_0} \ln \epsilon_r \nabla_t \mathcal{E}_{zi} \cdot \nabla_t \Phi_j \, dS \tag{18b}$$

$$\mathcal{W}_{ij} = -\int_{S-S_0} \ln \epsilon_r \nabla_t \mathcal{E}_{zi} \cdot \nabla_t \mathcal{E}_{zj} \, dS + (\kappa_j^e)^2 \int_{S-S_0} \ln \epsilon_r \mathcal{E}_{zi} \mathcal{E}_{zj} \, dS. \tag{18c}$$

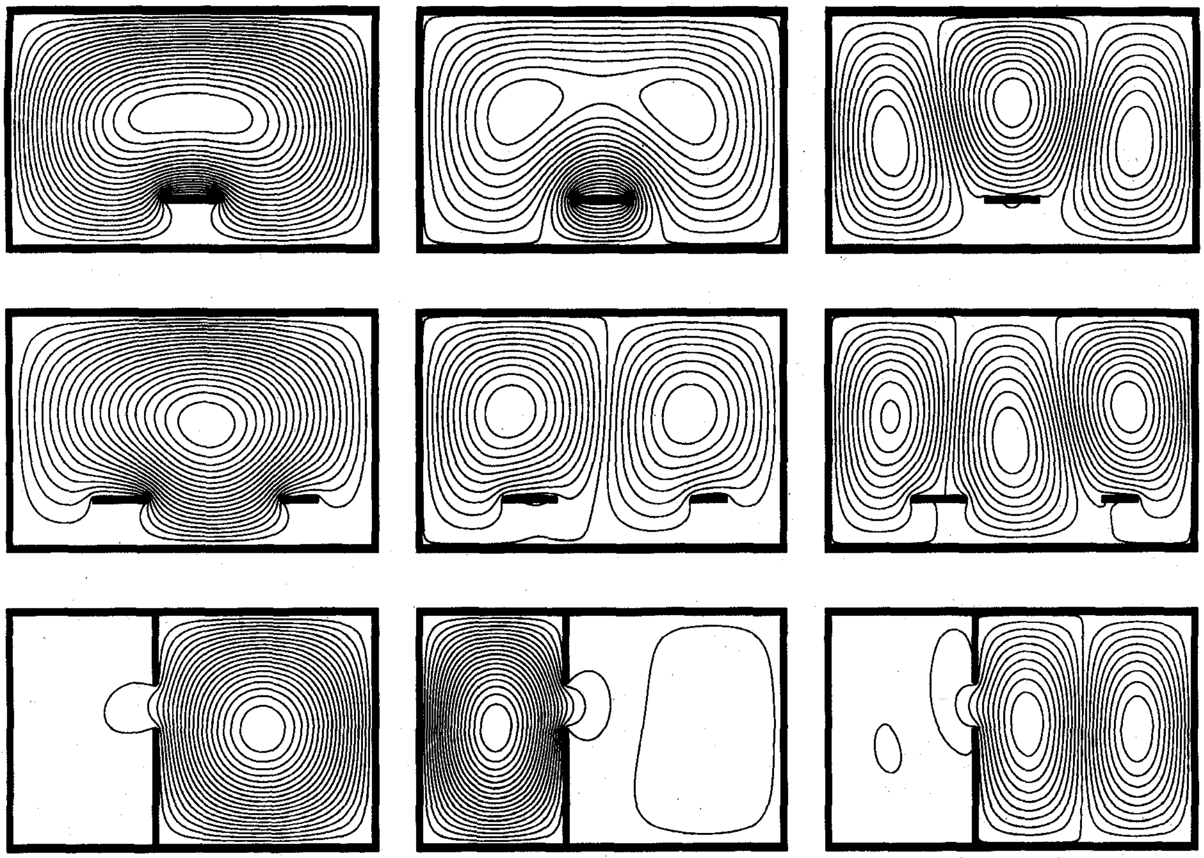

Fig. 3. Magnetic field lines of some TM-modes corresponding to a shielded strip line, two coupled strip lines, and a slot line.

Now the Rayleigh–Ritz procedure is applied. This results in a matrix eigenvalue problem for β^2

$$\begin{bmatrix} [\overline{\mathcal{R}}^{hh}] - [\tilde{\kappa}^h]^2 & [\overline{\mathcal{T}}]^t & [\overline{\mathcal{T}}^0] \\ [\overline{\mathcal{T}}] + [\tilde{\kappa}^e]^2[\mathcal{V}] & [\overline{\mathcal{R}}^{ee}] + [\tilde{\kappa}^e]^2([\mathcal{W}] - [I]) & [\overline{\mathcal{R}}^{e0}] + [\tilde{\kappa}^e]^2[\mathcal{W}^0] \\ [\overline{\mathcal{T}}^0] & [\overline{\mathcal{R}}^{e0}]^t & [\overline{\mathcal{R}}^{00}] \end{bmatrix} \begin{pmatrix} \boldsymbol{V}^H \\ \boldsymbol{V}^E \\ \boldsymbol{V}^0 \end{pmatrix} = (\tilde{\beta})^2 \begin{pmatrix} \boldsymbol{V}^H \\ \boldsymbol{V}^E \\ \boldsymbol{V}^0 \end{pmatrix}. \quad (19)$$

In comparison to (8) no coupling matrix appears at the right hand side of (19).

Let us consider the case that the dielectric constant ϵ_r changes abruptly. Then (16d) does not hold because the spatial derivative of neither $\boldsymbol{E}_t$ nor ϵ_r is regular while this is not the case for the product $\epsilon_r \boldsymbol{E}_t$. It can easily be shown that the eigenvectors of (8) and (19) are related by

$$\begin{pmatrix} \boldsymbol{U}^H \\ \boldsymbol{U}^E \\ \boldsymbol{U}^0 \end{pmatrix} = \begin{bmatrix} [\overline{\mathcal{R}}^{hh}] & [\overline{\mathcal{T}}]^t & [\overline{\mathcal{T}}^0]^t \\ [\overline{\mathcal{T}}] & [\overline{\mathcal{R}}^{ee}] & [\overline{\mathcal{R}}^{e0}] \\ [\overline{\mathcal{T}}^0] & [\overline{\mathcal{R}}^{e0}]^t & [\overline{\mathcal{R}}^{00}] \end{bmatrix} \begin{pmatrix} \boldsymbol{V}^H \\ \boldsymbol{V}^E \\ \boldsymbol{V}^0 \end{pmatrix}. \quad (20)$$

Using this transformation, (17b) can be reformulated to

$$\left\langle \frac{1}{\epsilon_r} \boldsymbol{\nabla}_t \times \boldsymbol{H}_t, \hat{\boldsymbol{k}} \boldsymbol{\nabla}_t \cdot \epsilon \boldsymbol{E}_t \right\rangle = (\boldsymbol{I}^E)^t [\tilde{\kappa}^e][\mathcal{S}][\tilde{\kappa}^e] \cdot ([\overline{\mathcal{T}}]\boldsymbol{V}^H + [\overline{\mathcal{R}}^{ee}]\boldsymbol{V}^E + [\overline{\mathcal{R}}^{e0}]\boldsymbol{V}^0). \quad (21)$$

Applying the Rayleigh–Ritz procedure in (14) again yields a modified matrix eigenvalue problem which can also be applied for abruptly changing dielectrics

$$\begin{bmatrix} [\overline{\mathcal{R}}^{hh}] - [\tilde{\kappa}^h]^2 & [\overline{\mathcal{T}}]^t & [\overline{\mathcal{T}}^0]^t \\ ([I] - [\tilde{\kappa}^e][\mathcal{S}][\tilde{\kappa}^e])[\overline{\mathcal{T}}] & ([I] - [\tilde{\kappa}^e][\mathcal{S}][\tilde{\kappa}^e])[\overline{\mathcal{R}}^{ee}] & ([I] - [\tilde{\kappa}^e][\mathcal{S}][\tilde{\kappa}^e])[\overline{\mathcal{R}}^{e0}] \\ [\overline{\mathcal{T}}^0] & [\overline{\mathcal{R}}^{e0}]^t & [\overline{\mathcal{R}}^{00}] \end{bmatrix} \begin{pmatrix} \boldsymbol{V}^H \\ \boldsymbol{V}^E \\ \boldsymbol{V}^0 \end{pmatrix} = (\tilde{\beta})^2 \begin{pmatrix} \boldsymbol{V}^H \\ \boldsymbol{V}^E \\ \boldsymbol{V}^0 \end{pmatrix}. \quad (22)$$

The expansion coefficients of the transverse magnetic field are related to those of the transverse electric field by

$$Z_0 \boldsymbol{I}^H = \tilde{\beta} \boldsymbol{V}^H \quad (23a)$$

$$Z_0 \boldsymbol{I}^E = \tilde{\beta}([I] - [\tilde{\kappa}^e][\mathcal{S}][\tilde{\kappa}^e])^{-1} \boldsymbol{V}^E \quad (23b)$$

$$Z_0 \boldsymbol{I}^0 = \tilde{\beta} \boldsymbol{V}^0. \quad (23c)$$

III. Numerical Results

The dispersion characteristics of dominant and higher order modes of various planar structures have been investigated by the eigenmode transformation technique. The convergence of the eigenmode transformation technique could be further improved by substituting the coupling matrices involving the integrand $1/\epsilon_r$ by the numerical inverse of its analytical inverse, which is given by replacing $1/\epsilon_r$ by ϵ_r as has been described in detail in [13].

Fig. 2 shows the convergence of the two eigenvalue formulations (8) and (9) for a shielded circular dielectric waveguide.

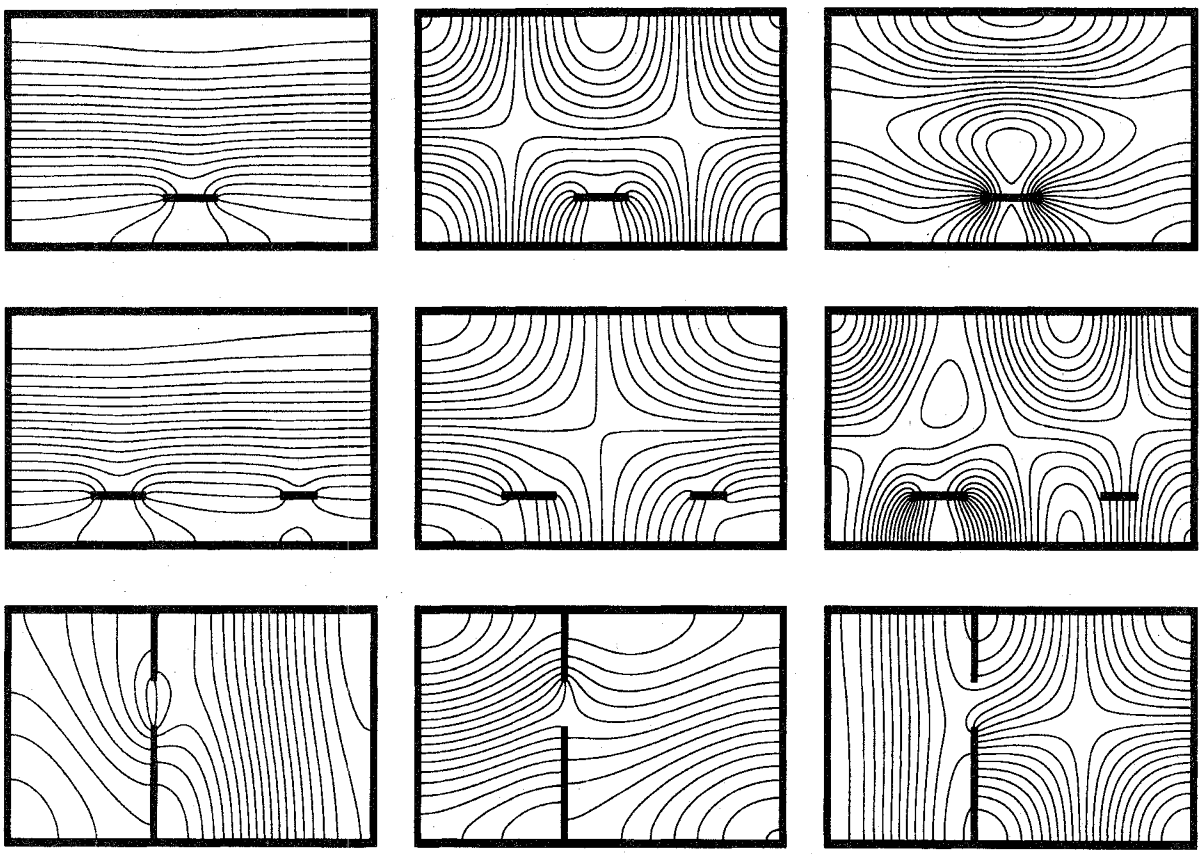

Fig. 4. Electric field lines of some TE-modes corresponding to a shielded strip line, two coupled strip lines and a slot line.

The relative error of β^2 of the dominant TE-mode with increasing number of expansion functions N is shown for two dielectric profiles, namely, for a dielectic rod with radius $R/R_s = 0.1$, where R_s is the radius of the shielding, and for a gaussian dielectric profile with a standard deviation of the same width. The maximum dielectric permittivity of the core is $\epsilon_r = 10$. Fig. 2 demonstrates that both approaches work well for smooth dielectric profiles. For abruptly changing dielectrics some field components are not continuous which leads to worse convergence because much more spectral terms need to be taken into account. Second, it is found that the eigenvalue formulation (19) has a much better convergence than (8). It is to be noted that for rotationally symmetric modes TE- and TM-contributions are decoupled in (19) and (8).

Figs. 3 and 4 show the magnetic (electric) field lines of some TM- (TE-)modes in a strip line, two coupled strip lines, and a slot line as a linear combination of the housing eigenmodes. This field representation provides the data necessary for the eigenmode transformation. The field lines have to be parallel (orthogonal) to the boundary and to the metal insert. This is in good agreement with the plots.

In Fig. 5 the cross sections of some shielded transmission lines which have the same substrate and therefore the same coupling matrices are plotted.The transformation matrices $[\mathcal{J}^{HH}]$, $[\mathcal{J}^{EH}]$, $[\mathcal{U}^{EE}]$, $[\mathcal{U}^{E0}]$, and $[\mathcal{U}^{L}]$, however, have to be determined for each structure, seperately. The eigenmode transformation of microstrip lines and coupled microstrip lines are computed by the methods presented in [8] while for the

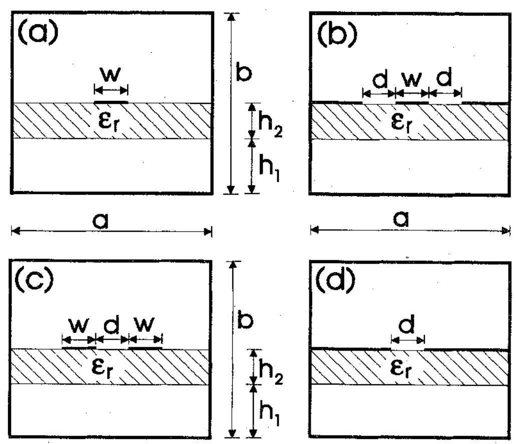

Fig. 5. Various shielded planar transmission lines with similar boundary conditions.

computation of the transformation matrices corresponding to finlines and coplanar lines the method suggested in [10] has been applied. Fig. 6 shows the cross section of a shielded dielectric image guide. For this structure no eigenmode transformation is necessary.

Fig. 7 shows the dispersion characteristics of the dominant modes of the planar transmission lines shown in Fig. 5 in comparison with the results of Yamashita and Atsuki ([14]). The agreement is good. Only for high dielectric permittivities ($\epsilon_r = 20$) there are small deviations. This can be explained by the fact that the bandwidth of the coupling matrices (7a)

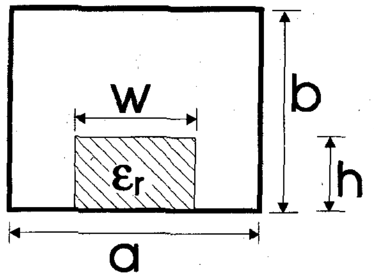

Fig. 6. Cross section of a dielectric image guide.

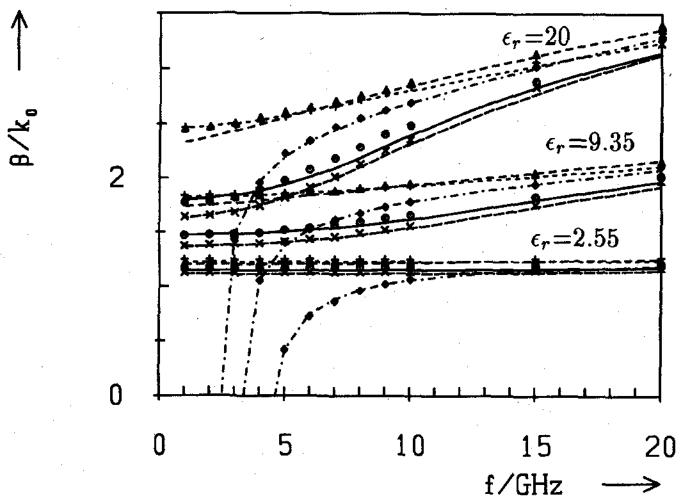

Fig. 7. Modal spectra of the dominant modes of the structures, shown in Fig. 5. Parameters: a = 20 mm, $w = d = 2$ mm, b = 10 mm, h_1 = 4.5 mm, h_2 = 1 mm.
Presented method: —, - - - -, · · ·, — —, — · —
Results of [14]: o, △, +, ×, ◇
correspond to (a), (b), odd mode of (c), even mode of (c), (d), respectively, in Fig. 5.; $\epsilon_r = 20, 9.35, 2.55$.

is larger for higher dielectric contrast which degrades the convergence of the infinite sums involved in the calculations.

Fig. 8 shows the modal spectrum of the shielded dielectric image guide shown in Fig. 6 as compared to the results of [15], [16]. In Figs. 8 and 9, positive values represent propagating modes (β is positive real) while negative values represent evanescent modes (β is negative imaginary). Four real modes and one pair of complex modes which splits into two real modes at a normalized frequency of about k_0a = 4.7 are plotted. One backward wave exists between k_0a = 4.7 and k_0a = 5.0. The agreement with the results of the program package MAFIA [16] is excellent, while the results of [15] are slightly different. This is especially valid for the frequency where the complex pair turns into two real eigenmodes.

The modal spectrum of a shielded microstrip line (two real eigenmodes forming a pair of complex modes between 16–25 GHz) is presented in Fig. 9. Our results are compared with those corresponding to the analysis presented in [6]. The agreement is excellent.

IV. Conclusion

Two proper matrix eigenvalue formulations for the analysis of shielded waveguides containing a dielectric and metal inserts have been proposed. The metal inserts are taken into account in form of linear transformations of the coupling matrices corresponding to the dielectric which makes the method modular. For shielded dielectric waveguides, the numerical implementation of both matrix eigenvalue formulations have been checked and compared to other methods. Various types of metal insert have been investigated and the validity of the transformation technique has been checked for various classes of planar transmission line.

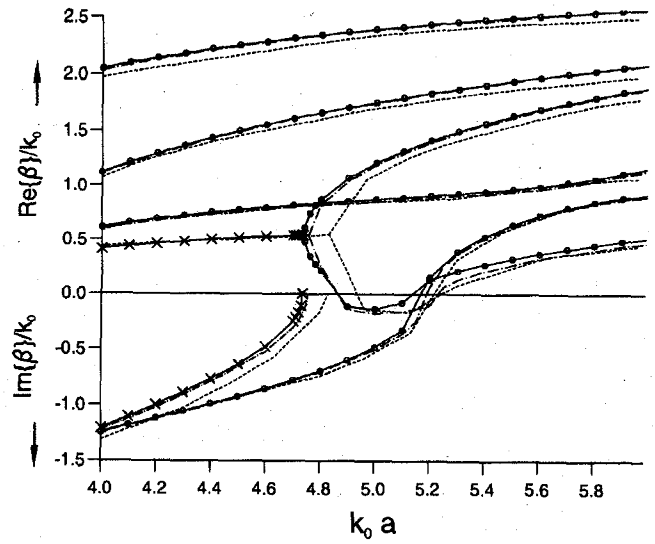

Fig. 8. Modal spectrum of a dielectric image guide. Parameter: a = 15.8 mm, w = 6.9 mm, b = 7.9 mm, h = 3.3 mm, ϵ_r = 9 —: presented method, o(×) calculated real (complex) modes, - -: results of [15], — · —: results of [16].

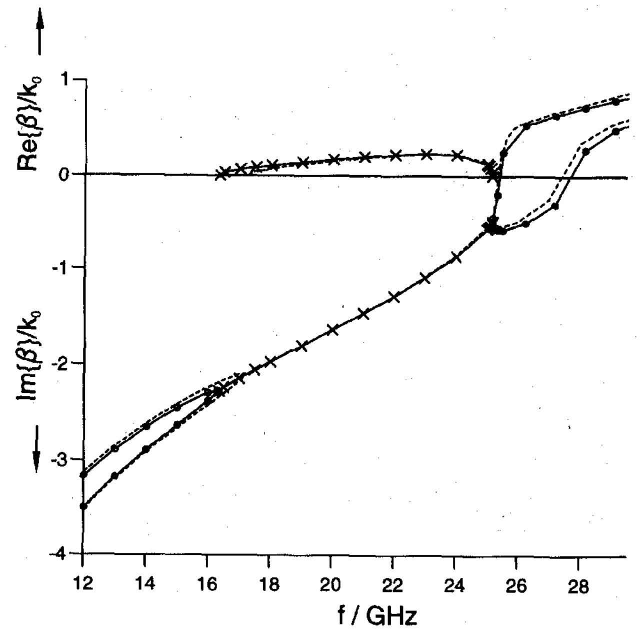

Fig. 9. Modal spectrum of a shielded microstrip line. Parameter: a = 10 mm, w = 1 mm, b = 5 mm, h_2 = 1 mm, $h_1 = 0, \epsilon_r = 10$. —: presented method, o(+) calculated real (complex) modes, - -: results of [6].

References

[1] A. S. Omar and K. Schünemann, "The effect of complex modes at finline discontinuities," *IEEE Trans. Microwave Theory Tech.*, vol. MTT-34, pp. 1508–1514, 1986.
[2] W. X. Huang and T. Itoh, "Complex modes in lossless shielded microstrip lines," *IEEE Trans. Microwave Theory Tech.*, vol. 36, pp. 163–165, 1988.

[3] C. J. Railton and T. Rozzi, "Complex modes in boxed microstrip," *IEEE Trans. Microwave Theory Tech.*, vol. 36, pp. 865–874, 1988.

[4] J.-T. Kuo and C.-K. C. Tzuang, "Complex modes in shielded suspended coupled microstrip lines," *IEEE Trans. Microwave Theory Tech.*, vol. 38, pp. 1278–1286, 1990.

[5] A. S. Omar and K. Schünemann, "Complex and backward-wave modes in inhomogeneously filled waveguides," *IEEE Trans. Microwave Theory Tech.*, vol. MTT-35, pp. 268–275, 1987.

[6] Y.-S. Xu and A. S. Omar, "Rigorous solution of mode spectra for shielded multilayer microstrip lines," *IEEE Trans. Microwave Theory Tech.*, vol. 42, pp. 1213–1222, 1994.

[7] R. E. Collin, *Foundations for Microwave Engineering.* New York: McGraw-Hill, 1966.

[8] A. S. Omar and K. Schünemann, "Analysis of waveguides with metal inserts," *IEEE Trans. Microwave Theory Tech.*, vol. 37, pp. 1924–1932, 1989.

[9] "Computation of cutoff wavenumbers of TE and TM modes in waveguides of arbitrary cross sections using a surface integral formulation," M. Swaminathan, E. Arvas, T. K. Sarkar, and A. R. Djordjević, *IEEE Trans. Microwave Theory Tech.*, vol. 38, pp. 154–159, 1990.

[10] A. S. Omar, A. Jöstingmeier, C. Rieckmann, and S. Lütgert, "Application of the GSD technique to the analysis of slot-coupled waveguides," *IEEE Trans. Microwave Theory Tech.*, vol. 42, pp. 2139–2148, 1994.

[11] W. C. Chew, *Waves and Fields in Inhomogeneous Media.* New York: Van Nostrand, 1990.

[12] W. C. Chew and M. A. Nasir, "A variational analysis of anisotropic inhomogeneous dielectric waveguides," *IEEE Trans. Microwave Theory Tech.*, vol. 37, pp. 661–668, 1989.

[13] A. S. Omar and A. Jöstingmeier, "Analytical inversion of a class of infinitely dimensioned matrices encountered in some microwave problems," *IEEE Microwave Guided Wave Lett.*, vol. 2, pp. 316–318, 1992.

[14] E. Yamashita and K. Atsuki, "Analysis of microstrip-like transmission lines by nonuniform discreization of integral equations," *IEEE Trans. Microwave Theory Tech.*, vol. MTT-24, pp. 195–200, 1976.

[15] J. Strube and F. Arndt, "Rigorous hybrid-mode analysis of the transition from rectangular waveguide to shielded dielectric image guide," *IEEE Trans. Microwave Theory Tech.*, vol. MTT-33, pp. 391–401, 1985.

[16] R. Klatt *et al.*, "MAFIA–three-dimensional electromagnetic CAD system for magnets, RF structures, and transient wake-field calculations," in *Proc. 1986 Linear Accelerator Conf. (Stanford Linear Accelerator Report)*, SLAC-303, pp. 276–278.

Christian Rieckmann was born May 16, 1968 in Hamburg, Germany. He received the Dipl.-Ing. degree in electrical engineering from the Technische Universität Hamburg–Harburg, Germany, in 1993.

Since 1993, he has been with the Arbeitsbereich für Hochfrequenztechnik at the Technische Universität Hamburg-Harburg as a Research Assistant. His current fields of research are concerned with electromagnetic field theory and high-power generation.

Andreas Jöstingmeier was born May 25, 1961 in Bielefeld, Germany. He received the Dipl.-Ing. degree in electrical engineering from the Technische Universität Braunschweig, Germany, in 1987 and the Doctor-Ing. degree from the Technische Universität Hamburg-Harburg, Germany, in 1991.

From 1987 to 1981, he worked as a Research Assistant at the Technische Universität Hamburg-Harburg where he was engaged in the investigation of dielectric resonators. From 1991 to 1995, he was with the Institut für Hochfrequenztechnik at the Technische Universität Braunschweig as a Research Assistant where he was concerned with numerical methods for microwave and millimeter-wave structures and high-power millimeter-wave tubes. In 1995, he joined the Machine Physics Division of DESY in Hamburg where he has been involved in the design of the S-Band Linear Collider.

A. S. Omar (M'87–SM'89), for a photograph and biography, see p. 944 of the June 1991 issue of this TRANSACTIONS.